Palestine Journal of Mathematics

Vol 14(Special Issue I)(2025) , 110–132

An Effectual Higher Order Computational Method for Treatment of Generalized Rosenau-KDV Equation

Ravneet Kaur and V.K.Kukreja

MSC 2010 Classifications: Primary 35G15; Secondary 35G46.

Keywords and phrases: Generalized Rosenau-KdV, compact finite difference method, SSP-RK43, stability analysis, eigenvalues.

The authors would like to thank the reviewers and editor for their constructive comments and valuable suggestions that improved the quality of our paper.

Corresponding Author: Ravneet Kaur

Abstract *This study evaluates a highly efficient compact finite difference method (CFDM6) for solving the generalized Rosenau-KdV equation numerically. It analyzes a nonstandard approach for discretizing spatial derivatives along with the strong stability preserving Runge-Kutta method (SSP-RK43) for time discretization to achieve optimized numerical results. To showcase the method's effectiveness and precision, error norms L_2 and L_∞ are calculated. Comparisons are made using several test problems with known exact solutions, as well as numerical solutions found in existing literature. The results are presented in tabular form to confirm that the numerical results are closely related to the exact solution.*

1 Introduction

Dispersive shallow water waves in lakes, canals, and along coastlines have long been a significant topic of study in fluid dynamics, especially in oceanography. The Korteweg-de-Vries (KdV) equation, the Boussinesq equation, the Peregrine equation, the regularised long wave (RLW) equation, the Kawahara equation, the Benjamin-Bona-Mahoney equation, and the Bona-Chen equation are just a few of the models that have been created using various hypotheses. Solutions including rogue waves, shock waves, solitary waves, and numerical solutions have been discussed in recent years. A number of models are reviewed and briefly summarised in this study, together with their approximate and analytical solutions.

The Korteweg-de Vries (KdV) equation is a prominent equation in mathematics and physics, recognized for its extensive applications in modeling wave propagation. The general form of the equation is expressed as:

$$\frac{\partial v}{\partial T} + \frac{\partial^2 v}{\partial x^3} + v\frac{\partial v}{\partial x} = 0. \tag{1.1}$$

Literature discusses various solutions to the Korteweg-de Vries (KdV) equation, including rational solutions, solitons, positons, negatons, breathers, complexitons, and interactions. Researchers have employed numerous techniques to derive both exact and numerical solutions, utilizing methods such as the multisymplectic structure of the KdV equation via the variational principle [1], differential quadrature methods based on Lagrange polynomials and cosine expansions [3]. Other approaches include the operator splitting method [4] and Painlevé analysis [5], as well as the quintic B-spline collocation method [6], Khater II as well as variational iteration methods [7], solitary wave solutions using trial equation method [8], polynomial conjecture in collaboration with rational solutions and rogue wave solutions [9].

The dynamics of dispersive shallow water waves have also been described by a number of

equations that have been published in the literature, including the Rosenau equation, sixth-order Boussinesq equation, Rosenau-Kawahara equation, Rosenau-KdV equation, Rosenau-RLW equation, and Rosenau-KdV-RLW equation. In contrast to the unidirectional KdV equation, Rosenau [10] proposed an equation for the dynamics of dense discrete systems in 1988 that addresses both wave-wave and wave-wall interactions. It is written as follows:

$$\frac{\partial v}{\partial T}+\frac{\partial v}{\partial x}+v\frac{\partial v}{\partial x}+\frac{\partial^5 v}{\partial x^4\partial T}=0. \tag{1.2}$$

Park [11, 12] discussed the existence and uniqueness of the solution to the Rosenau equation. The model was then thoroughly investigated using a variety of numerical techniques, such as the finite element Galerkin method [13, 14], finite difference approximation [15], orthogonal cubic spline collocation method [16], conservative finite difference schemes [17], high-order conservative difference schemes [18], mixed finite element methods [19], and radial basis function methods [20], among others.

The goal of the current study is to numerically solve the generalised Rosenau-KdV equation, which represents the discrete behaviour of shallow water waves. It is a linked form of equations (1.1) and (1.2). The following is the equation's generalised version.:

$$\frac{\partial v}{\partial T}+\alpha\frac{\partial v}{\partial x}+\beta\frac{\partial (v^p)}{\partial x}+\gamma\frac{\partial^3 v}{\partial x^3}+\frac{\partial^5 v}{\partial x^4\partial T}=0,\ \ (x,T)\in \Upsilon_x\times\Upsilon_T \tag{1.3}$$

$$v(x,0)=f(x),\ \ x\in\bar{\Upsilon}_x \tag{1.4}$$

$$\begin{aligned} v(A,T)&=v(B,T)=0,\\ v_x(A,T)&=v_x(B,T)=0,\quad T\in\bar{\Upsilon}_T\\ v_{xx}(A,T)&=v_{xx}(B,T)=0, \end{aligned} \tag{1.5}$$

In the above eq. (1.4) is the initial condition and eq. (1.5) are the conditions at the boundary. Also,the regions are $\Upsilon_x=(A,B)$, $\Upsilon_T=(T_0,T)$ and the variable $v(x,t)$ represents the nonlinear wave profile, $f(x)$ is a smooth function of $'x'$, coefficients α, β and γ are real valued functions and p is the power law nonlinearity. Observations give rise to the condition that $\lim_{T_0\to 0} u\to 0$ in almost all cases at $a\ll 0$ and $b\gg 0$, justifying the initial and boundary conditions given in eqs.(1.4) and (1.5) respectively are consistent with each other and reasonably agree to the assumptions made in eq.(1.5).

In published writings, methods such as sine-cosine and tanh method [21], solitary wave ansatz method [22], implicit finite difference method [23, 24], variational principle [25], subdomain method based on the sextic B-spline basis functions [26], finite element method based on collocation approach [27], conservative difference scheme [28], finite element method [29], splitting method with quintic B-spline collocation method [30], Crank-Nicolson meshless spectral radial point interpolation [31] and many other methods have been implemented depicting the exact and approximate solutions, polynomial scaling method[32].

In 1992, Lele [33] described a concise finite difference method that is simple, well-explained, and provides detailed information at smaller scales. This technique includes extra points for acquiring the derivatives. The concentration is computed separately at the boundary points, following either Neumann or Dirichlet conditions. Numerous researchers have utilized this numerical method to calculate solutions for a range of linear or nonlinear differential equations. The compact finite difference method is used in previous years to discuss various equations like reaction-diffusion [34], Poisson [35], Gross-Pitaevskii [36], convection-diffusion [37], fractional parabolic [38], Cattaneo Model [39], and Black-Scholes [40].

This study emphasizes an effective, very concise, and straightforward numerical method for addressing the generalized Rosenau-KdV equation. This study is motivated by the significance of using nonlinear partial differential equations that adhere to conservative laws. Based on the fundamental Taylor series, the sixth-order compact finite difference technique produces banded matrices. Afterward, the matrices can be integrated in time with minimal computational complexity using math software such as MATLAB, MATHEMATICA, etc. utilizing the SSP-RK43 scheme. The primary benefit of this approach is that it addresses nonlinear partial differential equations without the necessity of employing Hopf-Cole or similar transformations. The objective of this study is to utilize a proficient numerical method that incorporates higher order derivatives through the compact finite difference approach for both initial and boundary conditions, ensuring the highest level of convergence.

The remaining sections of this document are structured as follows: Section 2 provides a detailed introduction to the derivatives of the compact finite difference scheme. Section 3 involves executing the proposed scheme. The examination of the stability of the numerical method in Section 4 is carried out through the utilization of eigenvalues. In Section 5, two test problems are analyzed, where the error norms L_2 and L_∞ are computed and contrasted with existing numerical simulations in the literature. In Section 6, a concise summary is presented.

2 Introduction of derivatives with compact finite difference method

A detailed discussion is provided on the technique of the scheme applied for spatial interval $\bar{\Upsilon}_x = [A, B]$ and a time range $\bar{\Upsilon}_T = [T_0, T]$, with $T_0 = 0$. The fluid flow is partitioned into identical sections with uniform spacing intervals $x_i = A + ih$, where $i = 0, 1, 2, ..., N$, step size $Nh = B - A$, and time increment $\Delta T = T^{j+1} - T^j$, where $j = 0, 1, 2, ...$ and similarly $T^j = T_0 + j\Delta T$.

2.1 Spatial derivatives of first-order

The compact finite difference scheme at the inner nodal points is used exclusively to calculate first-order space derivatives in an implicit form [33] as:

$$\theta V'_{i-1} + V'_i + \theta V'_{i+1} = \mathfrak{a}\frac{V_{i+2} - V_{i-2}}{4h} + \mathfrak{b}\frac{V_{i+1} - V_{i-1}}{2h}, \tag{2.1}$$

where in simplified form $\mathfrak{a}$ equals one-third of the expression $4\theta - 1$, and $\mathfrak{b}$ equals two-thirds of the expression $2 + \theta$. Select the best value of parameter $\theta = \frac{1}{3}$ to achieve sixth-order accuracy, thus obtaining $\mathfrak{a} = \frac{1}{9}$ and $\mathfrak{b} = \frac{14}{9}$. Additionally, performing basic computations simplifies eq. (2.1) into tridiagonal matrix of sixth-order, with truncation error of $\frac{4}{7!}h^6 V_i^{(7)}$. The resulting generalized equation at interior points for $i = 2, 3, ..., N-2$ is given as:

$$V'_{i-1} + 3V'_i + V'_{i+1} = \frac{-V_{i-2} - 28V_{i-1} + 28V_{i+1} + V_{i+2}}{12h}. \tag{2.2}$$

For computing the derivative forward and backward schemes which are one-sided are used at points x_0, x_1, x_{N-1}, and x_N.

$$\begin{aligned}
V'_0 + 5V'_1 &= \frac{1}{60h}(-197V_0 - 25V_1 + 300V_2 - 100V_3 + 25V_4 - 3V_5),\\
2V'_0 + 11V'_1 + 2V'_2 &= \frac{1}{12h}(-80V_0 - 35V_1 + 136V_2 - 28V_3 + 8V_4 - V_5),\\
2V'_{N-2} + 11V'_{N-1} + 2V'_N &= \frac{1}{12h}(V_{N-5} - 8V_{N-4} + 28V_{N-3} - 136V_{N-2} + 35V_{N-1} + 80V_N),\\
5V'_{N-1} + V'_N &= \frac{1}{60h}(3V_{N-5} - 25V_{N-4} + 100V_{N-3} - 300V_{N-2} + 25V_{N-1} + 197V_N).
\end{aligned} \tag{2.3}$$

The matrix form of relations (2.2) and (2.3) are:

$$\mathbb{A}V' = \mathbb{B}V, \tag{2.4}$$

$$\begin{bmatrix} 1 & 5 & & & & & & \\ 2 & 11 & 2 & & & & & \\ & 1 & 3 & 1 & & & & \\ & & . & . & . & & & \\ & & . & . & . & & & \\ & & & . & . & . & & \\ & & & & 1 & 3 & 1 & \\ & & & & & 2 & 11 & 2 \\ & & & & & & 5 & 1 \end{bmatrix} \begin{bmatrix} V_0' \\ V_1' \\ V_2' \\ . \\ . \\ V_{N-2}' \\ V_{N-1}' \\ V_N' \end{bmatrix} = \frac{1}{h} \begin{bmatrix} -\frac{197}{60} & -\frac{25}{60} & \frac{300}{60} & -\frac{100}{60} & \frac{25}{60} & -\frac{3}{60} & & \\ -\frac{80}{12} & -\frac{35}{12} & \frac{136}{12} & -\frac{28}{12} & \frac{8}{12} & -\frac{1}{12} & & \\ -\frac{1}{12} & -\frac{28}{12} & 0 & \frac{28}{12} & \frac{1}{12} & & & \\ & . & . & . & & & & \\ & & . & . & . & & & \\ & & & & -\frac{1}{12} & -\frac{28}{12} & 0 & \frac{28}{12} & \frac{1}{12} \\ & & & \frac{1}{12} & -\frac{8}{12} & \frac{28}{12} & -\frac{136}{12} & \frac{35}{12} & \frac{80}{12} \\ & & & \frac{3}{60} & -\frac{25}{60} & \frac{100}{60} & -\frac{300}{60} & \frac{25}{60} & \frac{197}{60} \end{bmatrix}$$

2.2 Third-Order spatial derivative

Equally expressing the third derivative in a matrix format as:

$$\theta V_{i-1}''' + V_i''' + \theta V_{i+1}''' = \mathfrak{a}\frac{V_{i+3} - 3V_{i+1} + 3V_{i-1} - V_{i-3}}{8h^3} + \mathfrak{b}\frac{V_{i+2} - 2V_{i+1} + 2V_{i-1} - V_{i-2}}{2h^3}. \quad (2.5)$$

When $\theta = 0$ in the equation above, it signifies the explicit system to find the derivative. Considering $\theta = \frac{7}{16}$, the values of the parameters on right-hand side are evaluated generating $\mathfrak{a} = -\frac{1}{8}$ and $\mathfrak{b} = 2$. Therefore, the implicit method for calculating the third order derivative using a linear equation and a tridiagonal system, with a truncation error of $\frac{36}{9!}h^6V^9$, can be written as:

$$7V_{i-1}''' + 16V_i''' + 7V_{i+1}''' = \frac{1}{4h^3}\left(V_{i-3} - 64V_{i-2} + 125V_{i-1} - 125V_{i+1} + 64V_{i+2} - V_{i+3}\right). \quad (2.6)$$

In the same way as mentioned earlier, at the edge points the linear system is calculated as shown below.

$$\begin{aligned} h^3(V_0''' + 4V_1''') &= \frac{-109}{8}V_0 + 57V_1 - \frac{793}{8}V_2 + 94V_3 - \frac{423}{8}V_4 + 17V_5 \\ &\quad - \frac{19}{8}V_6, \\ h^3(V_0''' + 2V_1''' + V_2''') &= -10V_0 + 42V_1 - 74V_2 + 72V_3 - 42V_4 + 14V_5 - 2V_6, \\ \frac{h^3}{7}(4V_1''' + 7V_2''' + 4V_3''') &= -\frac{9}{8}V_0 - \frac{17}{7}V_1 - \frac{5}{8}V_2 - \frac{10}{7}V_3 + \frac{5}{8}V_4 - \frac{1}{7}V_5 - \frac{1}{56}V_6, \\ \frac{h^3}{7}(4V_{N-3}''' + 7V_{N-2}''' + 4V_{N-1}''') &= \frac{1}{56}V_{N-6} + \frac{1}{7}V_{N-5} - \frac{5}{8}V_{N-4} + \frac{10}{7}V_{N-3} + \frac{5}{8}V_{N-2} \\ &\quad + \frac{17}{7}V_{N-1} + \frac{9}{8}V_N, \\ h^3(V_{N-2}''' + 2V_{N-1}''' + V_N''') &= 2V_{N-6} - 14V_{N-5} + 42V_{N-4} - 72V_{N-3} + 74V_{N-2} \\ &\quad - 42V_{N-1} + 10V_N, \\ h^3(4V_{N-1}''' + V_N''') &= \frac{19}{8}V_{N-6} - 17V_{N-5} + \frac{423}{8}V_{N-4} - 94U_{N-3} \\ &\quad + \frac{793}{8}V_{N-2} - 57V_{N-1} + \frac{109}{8}V_N. \end{aligned} \quad (2.7)$$

In the matrix form:

$$\mathbb{C}V''' = \mathbb{D}V$$

where

$$\mathbb{C}V''' = \begin{bmatrix} 1 & 4 & & & & & & & & \\ 1 & 2 & 1 & & & & & & & \\ & 4 & 7 & 4 & & & & & & \\ & . & 7 & 16 & 7 & & & & & \\ & & & . & . & . & & & & \\ & & & & . & . & . & & & \\ & & & & & 7 & 16 & 7 & . & \\ & & & & & & 4 & 7 & 4 & \\ & & & & & & & 1 & 2 & 1 \\ & & & & & & & & 4 & 1 \end{bmatrix} \begin{bmatrix} V_0''' \\ V_1''' \\ V_2''' \\ V_3''' \\ . \\ . \\ V_{N-3}''' \\ V_{N-2}''' \\ V_{N-1}''' \\ V_N''' \end{bmatrix}$$

$$\mathbb{D}V = \frac{1}{h^3} \begin{bmatrix} -\frac{109}{8} & 57 & -\frac{793}{8} & 94 & -\frac{423}{8} & 17 & -\frac{19}{8} & & & & \\ -10 & 42 & -74 & 72 & -42 & 14 & -2 & & & & \\ -\frac{63}{8} & 17 & -\frac{35}{8} & -10 & \frac{35}{8} & 1 & -\frac{1}{8} & & & & \\ \frac{1}{4} & -16 & \frac{125}{4} & 0 & -\frac{125}{4} & 16 & -\frac{1}{4} & & & & \\ & & & . & . & . & & & & & \\ & & & . & . & . & & & & & \\ & & & \frac{1}{4} & -16 & \frac{125}{4} & 0 & -\frac{125}{4} & 16 & -\frac{1}{4} \\ & & & \frac{1}{8} & -1 & -\frac{35}{8} & 10 & \frac{35}{8} & -17 & \frac{63}{8} \\ & & & 2 & -14 & 42 & -72 & 74 & -42 & 10 \\ & & & \frac{19}{8} & -17 & \frac{423}{8} & -94 & \frac{793}{8} & -57 & \frac{109}{8} \end{bmatrix} \begin{bmatrix} V_0 \\ V_1 \\ V_2 \\ V_3 \\ . \\ . \\ V_{N-3} \\ V_{N-2} \\ V_{N-1} \\ V_N \end{bmatrix}$$

2.3 Fourth-Order spatial derivative

The fourth derivative obtained using the compact finite difference method with truncation error $\frac{193}{393120}h^6U^{10}$ *represented in the matrix form as follow:*

$$\begin{aligned} \theta V_{i-1}'''' + V_i'''' + \theta V_{i+1}'''' = \mathfrak{a}\frac{V_{i+3} - 9V_{i+1} + 16V_i - 9V_{i-1} + V_{i-3}}{6h^4} \\ + \mathfrak{b}\frac{V_{i+2} - 4V_{i+1} + 6V_i - 4V_{i-1} + V_{i-2}}{h^4}. \end{aligned} \tag{2.8}$$

In the above equation, setting $\theta = 0$ *results in an explicit method for calculating the derivative, while choosing* $\theta = \frac{7}{26}$ *gives an implicit scheme for the fourth-order derivative generating* $\mathfrak{a} = \frac{1}{13}$ *and* $\mathfrak{b} = \frac{19}{13}$*. Therefore, the corresponding tridiagonal system is expressed as:*

$$7V_{i-1}'''' + 26V_i'''' + 7V_{i+1}'''' = \left(\frac{V_{i-3} + 114V_{i-2} - 465V_{i-1} + 700V_i - 465V_{i+1} + 114V_{i+2} + V_{i+3}}{3h^4}\right). \tag{2.9}$$

For computation one-sided forward as well as backward schemes are considered at boundary points.

$$
\begin{aligned}
\frac{h^4}{6}(6V_0'''' + V_1'''') &= \frac{227}{36}V_0 - \frac{100}{3}V_1 + \frac{293}{4}V_2 - \frac{772}{9}V_3 + \frac{679}{12}V_4 - 20V_5 \\
&\quad + \frac{107}{36}V_6, \\
\frac{h^4}{12}(V_0'''' + 12V_1'''' + V_2'''') &= \frac{61}{18}V_0 - \frac{142}{9}V_1 + \frac{69}{2}V_2 - \frac{337}{9}V_3 + \frac{137}{6}V_4 - \frac{15}{2}V_5 \\
&\quad + \frac{19}{18}V_6, \\
\frac{h^4}{24}(V_1'''' + 24V_2'''' + V_3'''') &= -\frac{23}{36}V_0 - \frac{97}{6}V_1 + \frac{359}{6}V_2 - \frac{698}{9}V_3 + \frac{539}{12}V_4 - \frac{71}{2}V_5 \\
&\quad + \frac{13}{9}V_6, \\
\frac{h^4}{24}(V_{N-1}'''' + 24V_{N-2}'''' + V_{N-3}'''') &= \frac{13}{9}V_{N-6} - \frac{71}{2}V_{N-5} + \frac{539}{12}V_{N-4} - \frac{698}{9}V_{N-3} + \frac{359}{6}V_{N-2} \\
&\quad - \frac{97}{6}V_{N-1} - \frac{23}{36}V_N, \\
\frac{h^4}{12}((V_{N-2}'''' + 12V_{N-1}'''' + V_N'''') &= \frac{19}{18}V_{N-6} - \frac{15}{2}V_{N-5} + \frac{137}{6}V_{N-4} - \frac{337}{9}V_{N-3} + \frac{69}{2}V_{N-2} \\
&\quad - \frac{142}{9}V_{N-1} + \frac{61}{18}V_N, \\
\frac{h^4}{6}(V_{N-1}'''' + 6V_N'''') &= \frac{107}{36}107V_{N-6} - 20V_{N-5} + \frac{679}{12}V_{N-4} - \frac{772}{9}V_{N-3} + \frac{293}{4}V_{N-2} \\
&\quad - \frac{100}{3}V_{N-1} + \frac{227}{36}V_N.
\end{aligned}
\tag{2.10}
$$

In matrix form:

$$\mathbb{E}V'''' = \mathbb{F}V$$

$$
\mathbb{E}V'''' = \begin{bmatrix}
6 & 1 & & & & & & & \\
1 & 12 & 1 & & & & & & \\
 & 1 & 24 & 1 & & & & & \\
 & . & 7 & 26 & 7 & & & & \\
 & & & . & . & . & & & \\
 & & & & 7 & 26 & 7 & . & \\
 & & & & & 1 & 24 & 1 & \\
 & & & & & & 1 & 12 & 1 \\
 & & & & & & & 1 & 6
\end{bmatrix}
\begin{bmatrix} V_0'''' \\ V_1'''' \\ V_2'''' \\ V_3'''' \\ . \\ V_{N-3}'''' \\ V_{N-2}'''' \\ V_{N-1}'''' \\ V_N'''' \end{bmatrix}
$$

$$
\mathbb{F}V = \frac{2}{h^4}\begin{bmatrix}
\frac{227}{12} & -100 & \frac{879}{4} & \frac{-772}{3} & \frac{679}{4} & -60 & \frac{107}{12} & & & & \\
\frac{61}{3} & -\frac{284}{3} & 207 & -\frac{674}{3} & 137 & -45 & \frac{19}{3} & & & & \\
-\frac{23}{3} & -194 & 718 & \frac{2792}{3} & 539 & -426 & \frac{52}{3} & & & & \\
\frac{1}{6} & 19 & -\frac{155}{2} & \frac{350}{3} & -\frac{155}{2} & 19 & \frac{1}{6} & & & & \\
 & & & . & . & . & & & & & \\
 & & & . & . & . & & & & & \\
 & & & \frac{1}{6} & 19 & -\frac{155}{2} & \frac{350}{3} & -\frac{155}{2} & 19 & \frac{1}{6} \\
 & & & \frac{52}{3} & -426 & 539 & \frac{2792}{3} & 718 & -194 & -\frac{23}{3} \\
 & & & \frac{19}{3} & -45 & 137 & -\frac{674}{3} & 207 & -\frac{284}{3} & \frac{61}{3} \\
 & & & \frac{107}{12} & -60 & \frac{679}{4} & \frac{-772}{3} & \frac{879}{4} & -100 & \frac{227}{12}
\end{bmatrix}
\begin{bmatrix} V_0 \\ V_1 \\ V_2 \\ V_3 \\ . \\ . \\ V_{N-3} \\ V_{N-2} \\ V_{N-1} \\ V_N \end{bmatrix}
$$

3 CFDM6 Implementation

In the implementation process the first, third and fourth-order spatial derivatives are assigned the values as follows eq.(1):

$$(I+\mathbb{E}^{-1}\mathbb{F})V_T = -\alpha\mathbb{A}^{-1}\mathbb{B}V - \beta pV^{p-1}\mathbb{A}^{-1}\mathbb{B}V - \gamma\mathbb{C}^{-1}\mathbb{D}V,$$

$$\mathcal{M}V_T = (-\alpha\mathbb{A}^{-1}\mathbb{B} - \beta pV^{p-1}\mathbb{A}^{-1}\mathbb{B} - \gamma\mathbb{C}^{-1}\mathbb{D})V \equiv \mathcal{L}'V,$$

$$V_T \equiv \mathcal{L}V, \tag{3.1}$$

where $\mathcal{M} = I+\mathbb{E}^{-1}\mathbb{F}$ and $\mathcal{L} = \mathcal{M}^{-1}\mathcal{L}'$ is a nonlinear differential operator.

3.1 SSP-RK43 scheme

The system of ODEs (3.1) is solved using the SSP-RK43 scheme, which advances the temporal value from the T^j to T^{j+1} level through the following operations:

$$\begin{aligned}
V^{(1)} &= V^j + \frac{\Delta T}{2}\mathcal{L}(V^j),\\
V^{(2)} &= V^{(1)} + \frac{\Delta T}{2}\mathcal{L}(V^{(1)}),\\
V^{(3)} &= \frac{2}{3}V^j + \frac{1}{3}V^{(2)} + \frac{\Delta T}{6}\mathcal{L}(V^{(2)}),\\
V^{j+1} &= V^{(3)} + \frac{\Delta t}{2}\mathcal{L}(V^{(3)}).
\end{aligned} \tag{3.2}$$

Using beginning condition, value of $V(x,t)$ at each time measure can be calculated.

4 Convergence and Stability

A thorough examination of the reliability and convergence characteristics of SSP-RK43 follows below. The differential equation $\mathcal{L}V = \lambda V$, where λ is the eigenvalue, given as:

$$\frac{dV}{dT} = \mathcal{L}V_i = \lambda V_i. \tag{4.1}$$

with the assumption that $\mathcal{L}$ is relatively invariant in the domain. The approximate solution is obtained in terms of recursive method for $T^{j+1} = T^j + \Delta T$ as:

$$V(T) = \exp(\lambda\Delta T)^j V^0.$$

On applying the SSP-RK43 method to the Eq. (4.1) the following form of solution is obtained:

$$V(T) = C_1[E(\lambda\Delta x)]^j,$$

where the constant C_1 is determined from the initial condition and an approximation of $(\exp(\lambda\Delta T)$ is considered as $E(\lambda\Delta T)$. From the aspect of stability analysis, the absolute stability $|E(\lambda\Delta T)| \leq 1$ and for relative stability $|E(\lambda\Delta T)| \leq \exp(\lambda\Delta T)$.

The following form is obtained:

$$\begin{aligned}
V^1 &= V^j + \frac{\Delta T}{2}\lambda V^j = \left(I + \frac{\Delta T}{2}\lambda\right)V^j,\\
V^2 &= V^1 + \frac{\Delta T}{2}\lambda V^1 = \left(I + \frac{\Delta T}{2}\lambda\right)V^1,\\
V^3 &= \frac{2}{3}V^j + \frac{1}{3}V^2 + \frac{\Delta T}{6}\lambda V^2 = \frac{2}{3}V^j + \frac{1}{3}\left(I + \frac{\Delta T}{2}\lambda\right)V^2,\\
V^{j+1} &= V^3 + \frac{\Delta T}{2}\lambda V^3 = \left(I + \frac{\Delta T}{2}\lambda\right)V^3.
\end{aligned}$$

Applying backward substitutions and taking norm, the following equation is obtained:

$$V^{j+1} = \left[I + \frac{\Delta T}{2}\mathcal{L} + \frac{1}{2!}\left(\frac{\Delta T}{2}\mathcal{L}\right)^2 + \frac{1}{3!}\left(\frac{\Delta T}{2}\mathcal{L}\right)^3 + \frac{1}{4!}\left(\frac{\Delta T}{2}\mathcal{L}\right)^4\right]V^{(j)}.$$

Thus, the growth factor for SSP-RK43 is:

$$E(\lambda\Delta t) = \left[I + \frac{\Delta T}{2}L + \frac{1}{2!}\left(\frac{\Delta T}{2}\mathcal{L}\right)^2 + \frac{1}{3!}\left(\frac{\Delta T}{2}\mathcal{L}\right)^3 + \frac{1}{4!}\left(\frac{\Delta T}{2}\mathcal{L}\right)^4\right].$$

If $\frac{\Delta T}{2}\lambda > 0$, *then* $\exp(\frac{\Delta T}{2}\lambda) \geq E(\frac{\Delta T}{2}\lambda)$, *clearly showing SSP-RK43 always relatively stable. For obtaining the absolute stability corresponding to* $\frac{\Delta T}{2}\lambda < 0$, *the interval is computed using graphical plot between* $|E(\frac{\Delta T}{2}\lambda)|$ *and* $(\frac{\Delta T}{2}\lambda)$ *[42]. The resulting interval of the absolute stability is* $-2.78 < \frac{\Delta T}{2}\lambda < 0$.

$$\exp(\mathcal{L}\frac{\Delta T}{2}) = I + \mathcal{L}t + \frac{(\mathcal{L}\frac{\Delta T}{2})^2}{2!} + \frac{(\mathcal{L}\frac{\Delta T}{2})^3}{3!} + ...$$

The transformation matrix $\mathcal{P}$ *is considered to diagonalise* $\mathcal{L}$ *that results* $\mathcal{P}^{-1}\mathcal{L}\mathcal{P} = \mathcal{D}$, *where* $\mathcal{D}$ *is the diagonal matrix, obtaining the relation as:*

$$\mathcal{P}^{-1}\exp\left(\mathcal{L}\frac{\Delta T}{2}\right)\mathcal{P} = \exp\left(\mathcal{D}\frac{\Delta T}{2}\right), \tag{4.2}$$

where

$$\mathcal{D} = \begin{bmatrix} \lambda_1 & & & & & \\ & \lambda_2 & & & & \\ & & . & . & . & \\ & & . & . & . & \\ & & & & \lambda_{n-1} & \\ & & & & & \lambda_n \end{bmatrix}.$$

and n *depends on the time domain. Let* $\mathcal{P}^{-1}U = v$ *in eq. (4.1), the differential equation becomes:*

$$\frac{dv}{dt} = \mathcal{D}v.$$

The solution of this equation is $v = \exp(\mathcal{D}\Delta T)v_0$ *and the following recursive relation is obtained:*

$$v^{j+1} = E(\mathcal{D}\Delta T)v^j. \tag{4.3}$$

For this system, the term $E(\mathcal{D}\Delta T)$ *is an approximation to* $\exp(\mathcal{D}\Delta T)$. *Each diagonal element of* $E^j(\lambda^j\Delta T)$ *is an approximation to the diagonal elements of* $\exp(\mathcal{D}\Delta T)$. *From Eq. (4.1), as discussed will be absolutely stable if:*

$$|E^j(\lambda_j\Delta T)| < 1, \quad j = 1, 2, .., n, .. \tag{4.4}$$

The stability region on the domain of a $\lambda\Delta T$*-complex plane is, for which* $\left|\frac{V^{j+1}}{V^j}\right| \leq 1$. *To compute the stability region over the complex plane of eq. (4.1) using SSP-RK43, the coefficients of the matrix are:*

$$\sum_{m=0}^{4}\frac{(\mathcal{L}\Delta T)^m}{m!},$$

and the eigenvalues of the matrix are:

$$\sum_{m=0}^{4}\frac{(\lambda\Delta T)^m}{m!}.$$

Also, a graph is plotted for SSP-RK43 scheme with third order of convergence given in Figure 1.

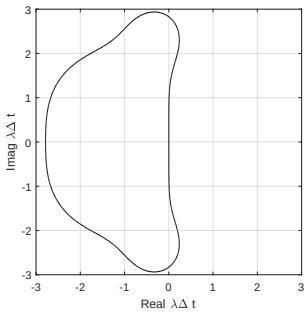

Figure 1: Stability region of SSP-RK43

4.1 Stability conditions

Based on the information provided above, the following are the necessary conditions that the eigenvalues of $\mathcal{L}$ should satisfy for stability:

From the above theorems, the following given below [42] are the concluding conditions:

- *For real λ_j : $-2.78 < \Delta t\lambda_j < 0$,*
- *For pure imaginary λ_j : $-2\sqrt{2} < \Delta t\lambda_j < 2\sqrt{2}$,*
- *For complex λ_j : $\Delta t\lambda_j$ should lie in the region, as given by [43].*

4.2 Analysis for Convergence

For the convergence investigation of SSP-RK43 method, consider the ordinary differential eq. (4.1).

Theorem 4.1. *The assumption is that a given IVP, $\frac{\partial V}{\partial T} = \mathcal{L}(V)$, has a unique solution if the function $\mathcal{L}(V)$ complies with the following conditions:*

- *$\mathcal{L}(V)$ is a real function.*
- *$\mathcal{L}(V)$ is well defined and continuous in the domain of $T \in \Phi_T$ and $V \in (-\infty, \infty)$.*
- *There exist a constant called Lipschitz constant κ such that*

$$|\mathcal{L}(V, T, \Delta T) - \mathcal{L}(\dot{V}, T, \Delta T)| \leq \kappa |V - \dot{V}|,$$

where $T \in \Phi_T$ and V and $\dot{V}$ be any two different points.

Lemma 4.2. *If the incremental function $\phi(V, T, \Delta T)$ satisfy the conditions given below then one-step method is said to be regular.*

(i) The function is continuous and is well defined over the stipulated space and time domain.

(ii) For all $T \in \Phi_T$ and $V, \dot{V} \in (-\infty, \infty)$ there exits a constant κ such that:

$$|\phi(V, T, \Delta T) - \phi(\dot{V}, T, \Delta T)| \leq \kappa |V - \dot{V}|. \tag{4.5}$$

Lemma 4.3. *A one-step method is considered consistent if $\phi(V, T, 0) = \mathcal{L}(V, T)$.*

Theorem 4.4. *The necessary and sufficient condition for the convergence with the order (say) $p \geq 1$ of a regular single step method is consistency.*

Proof. Consider a specific incremental function $\phi(V, T, \Delta T)$. Assume that the given differential equation $V_T \equiv \mathcal{L}V$ has a unique solution $V(T)$ on Φ_T and also $V(T) \in C^{(p+1)}\Phi_T$ for $p \geq 1$. Using the Taylor's series expansion about any point T^j:

$$V(T) = V(T^j) + (T - T^j)V^{(1)}(T^j) + \frac{1}{2!}(T - T^j)^2 V^{(2)}(T^j) + ... + \frac{1}{p!}(T - T^j)^p V^p(T^j)$$
$$+ \frac{1}{(p+1)!}(T - T^j)^{p+1} V^{p+1}(\xi^j),$$

where $\xi \in (T^j, T)$. Taking $T = T^{j+1}$ one gets:

$$V(T^{j+1}) - V(T^j) = \Delta t V^{(1)}(T^j).$$

Thus, the incremental function is defined as:

$$\phi(V(T^j), T^j, \Delta T) = \Delta T V^{(1)}(T^j) + \frac{1}{2!}(\Delta T)^2 V^{(2)}(T^j) + ... + \frac{1}{p!}(\Delta T)^p V^{(p)}(T^j).$$

Evaluating the numerical value V^j alongwith the exact value $v(T^j)$. Hence, the value of $V^{j+1} = V^j + \Delta T \phi(V(T^j), T^j, \Delta T),\ \ j = 0, 1, 2, ..., n-1$. This helps in computed error using Taylor's series as:

$$V^{j+1} = V^j + \Delta t V^{(1)^j} + \frac{\Delta T^2}{2!} V^{(2)^j} + \frac{\Delta T^3}{3!} V^{(3)^j} + ... + \frac{\Delta T^p}{p!} V^{pj} + \frac{\Delta T^{p+1}}{(p+1)!} V^{p+1}(\xi)^j.$$

The method SSP-RK43 approximates the value using the following relations as:

$$V^{j+1} = V^j + \Delta t \mathcal{L}(V^j) + \frac{\Delta T^2}{2!}\mathcal{L}^2(V^j) + \frac{\Delta T^3}{3!}\mathcal{L}^3(V^j) + ... + \frac{\Delta T^p}{p!}\mathcal{L}^p(V^j).$$

The following relation is obtained:

$$\Delta T \phi(V(T^j), T^j, \Delta T) = \Delta T V^{(1)}(t^j) + \frac{\Delta T^2}{2!}\mathcal{L}^2(V^j) + \frac{\Delta T^3}{3!}\mathcal{L}^3(V^j) + ... + \frac{\Delta T^p}{p!}\mathcal{L}^p(V^j) \quad (4.6)$$

The value of $\Delta t \phi(V^j, T^j, \Delta T)$ is obtained from $\Delta T \phi(v(T^j), T^j, \Delta T)$ by using the numerical value of V^j instead of the precise value $v(T^j)$. The numerical value of $V(T^{j+1})$ using SSP-RK43, is as follow:

$$V^{j+1} = V^j + \Delta T \phi(V^j, T^j, \Delta T) + \frac{\Delta T^2}{2!}\phi'(V^j, T^j, \Delta T) + \frac{\Delta T^3}{3!}\phi''(V^j, T^j, \Delta T) + ...$$

For the above relation, the values of $V(T^j), V^{(1)}(T^j), V^{(2)}(T^j)...V^p(T^j)$ are computed as follows:

$$\begin{aligned} V^{(1)}(T^j) &= \mathcal{L}(V(T^j), t^j) \\ V^{(2)}(T^j) &= \mathcal{L}_T + \mathcal{L}\mathcal{L}_V \\ V^{(3)}(T^j) &= \mathcal{L}_{TT} + 2'\mathcal{L}_{TV} + \mathcal{L}^2 L_{VV} + L_V(\mathcal{L}_T + \mathcal{L}\mathcal{L}_V) \\ &... \end{aligned}$$

The error term is obtained from these computed values at T^j as:

$$\frac{\Delta t^{p+1}}{(p+1)!} V^{p+1}(\xi^j) \ < \ \epsilon. \quad (4.7)$$

Hence on simplifying:

$$\Delta t^{p+1} V^{p+1}(\xi^j) \ < \ \epsilon(p+1)!.$$

In other words,

$$\Delta t^{p+1} \mathcal{L}^p(\xi^j) \ < \ \epsilon(p+1)!. \quad (4.8)$$

Thus, the considering value of p obtains an upper bound. It is observed that for calculation purposes, the $\mathcal{L}^p(\xi^j)$ in eq. (4.8) is swapped with $max|\mathcal{L}^p(\xi^j)|$ in the time domain Φ_T. The SSP-RK43 scheme described above can be rewritten as follows:

$$\begin{aligned} Q_1 &= V^j + \frac{\Delta T}{2}\mathcal{L}(V^j, t^j), \\ Q_2 &= Q_1 + \frac{\Delta T}{2}\mathcal{L}(Q_1), \\ Q_3 &= \frac{2}{3}V^j + \frac{1}{3}Q_2 + \frac{\Delta T}{6}\mathcal{L}(Q_2), \\ V^{j+1} &= Q_3 + \frac{\Delta T}{2}\mathcal{L}(Q_3). \end{aligned} \quad (4.9)$$

The rewritten form of iterated value of V^{j+1} in convex combination of function as follows:

$$V^{j+1} = V^j + c_1Q_1 + c_2Q_2 + c_3Q_3. \tag{4.10}$$

Taylor's series expansion shapes the incremental function as:

$$\phi(V^j, T^j, \Delta T) = (\Delta T)^{-1}(c_1Q_1 + c_2Q_2 + c_3Q_3) \tag{4.11}$$

Convergence in an elaborated form is described below:

$$\begin{aligned} Q_1 - Q_1{}^* &= V^j + \frac{\Delta t}{2}\mathcal{L}(V^j) - V^{j*} + \frac{\Delta T}{2}\mathcal{L}(V^{j*}) \\ |Q_1 - Q_1{}^*| &\leq |V^j - V^{j*}| + \frac{\Delta T}{2}|\mathcal{L}(V^j) - \mathcal{L}(V^{j*})| \\ &\leq (1 + \frac{\Delta T}{2}\kappa)|V^j - V^{j*}|. \end{aligned}$$

$$\begin{aligned} Q_2 - Q_2{}^* &= Q_1 + \frac{\Delta T}{2}\mathcal{L}(Q_1) - Q_1{}^* - \frac{\Delta T}{2}\mathcal{L}(Q_1{}^*) \\ |Q_2 - Q_2{}^*| &\leq |Q_1 - Q_1{}^*| + \frac{\Delta T}{2}|\mathcal{L}(Q_1) - \mathcal{L}(Q_1{}^*)| \\ &= |Q_1 - Q_1{}^*| + \frac{\Delta T}{2}|\mathcal{L}\left(V^j + \frac{\Delta T}{2}\mathcal{L}(V^j)\right) - \mathcal{L}\left(V^{j*} + \frac{\Delta T}{2}\mathcal{L}(V^{j*})\right)| \\ &\leq \left(1 + \frac{\Delta T}{2}\kappa\right)|V^j - V^{j*}| + \frac{\Delta T}{2}\Bigg[\mathcal{L}(V^j) + \frac{\Delta T}{2}\mathcal{L}(V^j)\mathcal{L}_V(V^j) \\ &+ \left(\frac{\Delta T}{2}\mathcal{L}(V^j)\right)^2\mathcal{L}_{VV}(V^j) + ... - \mathcal{L}(V^{j*}) - \frac{\Delta T}{2}\mathcal{L}(V^{j*})\mathcal{L}_V(V^{j*}) \\ &- \left(\frac{\Delta T}{2}\mathcal{L}(V^{j*})\right)^2\mathcal{L}_{VV}(V^{j*})\Bigg] \\ &\leq \left(1 + \frac{\Delta T}{2}\kappa\right)|V^j - V^{j*}| + \frac{\Delta T}{2}\left[\mathcal{L}(V^j) - \mathcal{L}(V^{j*})\right] \\ &+ \left(\frac{\Delta T}{2}\right)^2|\mathcal{L}(V^j)\mathcal{L}_V(V^j) - \mathcal{L}(V^{j*})\mathcal{L}_V(V^{j*})| \\ &+ \left(\frac{\Delta T}{2}\right)^3|(\mathcal{L}(V^j))^2\mathcal{L}_{VV}(V^j) - (\mathcal{L}(V^{j*}))^2\mathcal{L}_{VV}(V^{j*})| + ... \\ &\leq (1 + \Delta t\kappa)|V^j - V^{j*}| + \left(\frac{\Delta T}{2}\right)^2(\kappa)^2|V^j - V^{j*}| \\ &= \left[1 + \Delta t\kappa + \left(\frac{\Delta T}{2}\kappa\right)^2\right]|V^j - V^{j*}|. \end{aligned}$$

$$
\begin{aligned}
Q_3 - {Q_3}^* &= \frac{2}{3}V^j + \frac{Q_2}{3} + \frac{\Delta T}{2}\mathcal{L}(Q_2) - \frac{2}{3}V^{j^*} - \frac{{Q_2}^*}{3} - \frac{\Delta t}{2}\mathcal{L}({Q_2}^*))\\
|Q_3 - {Q_3}^*| &= \frac{2}{3}|V^j - V^{j^*}| + \frac{1}{3}|Q_2 - {Q_2}^*| + \frac{\Delta T}{2}|\mathcal{L}(Q_2) - \mathcal{L}({Q_2}^*)|\\
&\leq \frac{2}{3}|V^j - V^{j^*}| + \frac{1}{3}|Q_2 - {Q_2}^*| + \left|\frac{\Delta T}{2}\left[\mathcal{L}(Q_1 + \frac{\Delta T}{2}\mathcal{L}(Q_1)) - \mathcal{L}(Q_1^* + \frac{\Delta T}{2}\mathcal{L}(Q_1^*))\right]\right|\\
&\leq \frac{2}{3}|V^j - V^{j^*}| + \frac{1}{3}|Q_2 - {Q_2}^*|\\
&+ \frac{\Delta T}{2}\left[|(\mathcal{L}(V^j) - \mathcal{L}(V^{j^*}))| + \frac{\Delta T}{2}|\mathcal{L}(V^j)\mathcal{L}_V(V^j) - \mathcal{L}_V(V^{j^*})|\right]\\
&\leq |V^j - V^{j^*}| + \frac{\Delta T}{2}\kappa(2 + \frac{\Delta T}{2}\kappa)|V^j - V^{j^*}| + \frac{\Delta T}{2}\kappa|V^j - V^{j^*}| + \left(\frac{\Delta T}{2}\kappa\right)^2|V^j - V^{j^*}|\\
&\leq |V^j - V^{j^*}| + \left[\frac{3\Delta T}{2}\kappa + 2\left(\frac{\Delta T}{2}\kappa\right)^2\right]|V^j - V^{j^*}|.
\end{aligned}
$$

The free parameters [42] are adjusted to a high value based on absolute stability range. Another option is to reduce the overall amount of the absolute values of the truncation error coefficients. This obtains, $\mathcal{L}_V < \kappa$ and $\mathcal{L}_{VV} < \frac{\kappa^2}{M}$ where M is the convergence upper bound. The incremental function is analyzed below:

$$
\begin{aligned}
|\phi(V^j, T^j, \Delta T) - \phi(V^{j^*}, T^j, \Delta T)| &= (\Delta T)^{-1}|c_1Q_1 + c_2Q_2 + c_3Q_3 - c_1{Q_1}^* - c_2{Q_2}^* - c_3{Q_3}^*|\\
&= (\Delta T)^{-1}(c_1|Q_1 - {Q_1}^*| + c_2|Q_2 - {Q_2}^*| + c_3|Q_3 - {Q_3}^*|)\\
&\leq (\Delta T)^{-1}\left[c_1\left(1 + \frac{\Delta T}{2}\kappa\right)|V^j - V^{j^*}|\right.\\
&+ c_2\left(\left[1 + \Delta T\kappa + \left(\frac{\Delta T}{2}\kappa\right)^2\right]|V^j - V^{j^*}|\right)\\
&\left.+ c_3\left(|V^j - V^{j^*}| + \left[\frac{3\Delta T}{2}\kappa + 2\left(\frac{\Delta T}{2}\kappa\right)^2\right]|V^j - V^{j^*}|\right)\right]\\
&\leq \left[(\Delta T)^{-1}(c_1 + c_2 + c_3) + \left[c_1 + 2c_2 + c_3\right]\frac{\kappa}{2}\right.\\
&\left.+ \left[c_2 + 2c_3\right]\Delta T\left(\frac{\kappa}{2}\right)^2\right]|V^j - V^{j^*}|.
\end{aligned}
$$

The backward substitution of eq. (4.9) along with its contrast with Taylor's series [42] gives $c_1 = \frac{1}{4},\ c_2 = \frac{1}{2},\ c_3 = \frac{1}{4}$. Hence an inequality is obtained as:

$$
|\phi(V^j, T^j, \Delta T) - \phi(V^{j^*}, T^j, \Delta T)| \leq \kappa\left(1 + \frac{1}{2}\Delta T\kappa + \frac{1}{6}(\Delta T\kappa)^2\right)|V^j - V^{j^*}|.
$$

It is observed that $|\phi(V^j, T^j, \Delta T)|$ justifies the Lipschitz condition in V^j moreover also a continuous function in ΔT. Hence, SSP-RK43 is convergent. □

4.3 Implementation of Stability Analysis

For analyzing the stability of the model consider maxV = m (say) in eq.(1), to handle the nonlinearity factor as:

$$
V_T = \mathcal{M}^{-1}(-\alpha\mathbb{A}^{-1}\mathbb{B} - \beta pm^{p-1}\mathbb{A}^{-1}\mathbb{B} - \gamma\mathbb{C}^{-1}\mathbb{D})V \equiv PV. \tag{4.12}
$$

The eigenvalues of the coefficient matrix P are the sole factors determining the stability of the system. The conditions [42] that eigenvalues of $\mathcal{P}$ must fulfill are outlined below:
(i) For real σ_i : $-2.78 < \Delta T\sigma_i < 0$,

(ii) For pure imaginary σ_i *:* $-2\sqrt{2} < \Delta T\sigma_i < 2\sqrt{2}$,
(iii) For complex σ_i *:* $\Delta T\sigma_i$ *should lie in the region as given by [43].*

In Figure 2 and Figure 3, graphical representation of eigenvalues of coefficient matrix P *corresponding to problem 1 and problem 2 of generalized Rosenau-KdV equation with different values of parameter* $h = 0.1, 0.2, 1, 2$ *for the time* $T = 20$ *is shown. It is observed that the eigenvalues of both the problems are highly compatible with above said conditions, therefore it can be concluded that CFDM6 is a stable numerical technique.*

5 Numerical Experiments

In this section, the accuracy and efficacy of the compact finite difference method is measured for a couple of problems. Tabular form of the numerical results and exact solution is presented. The accuracy of the method is shown graphically with the help of figures. Mass and energy conservation properties are also considered to justify the validity of the proposed technique, which are given as follows:

$$\mathcal{Q}(T) = \int_A^B v(x,t)dx = \int_A^B v(x,0)dx = \mathcal{Q}(0) \backsimeq h\sum_{i=1}^{N} V_i$$

$$\mathcal{E}(T) = \int_A^B [v^2 + v_{xx}^2]dx = \mathcal{E}(0) \backsimeq h\sum_{i=1}^{N} V_i^2 + (V_{xx})_i^2$$

Effectiveness of the proposed method is clearly shown by L_2 *and* L_∞ *error norms using following relation:*

$$L_\infty = \|v_i - V_i\|_\infty = \max_{0\le i\le N} |v_i - V_i|, \qquad L_2 = \|v_i - V_i\|_2 = \sqrt{h\sum_{i=0}^{N}(\mathbb{V}_i - V_i)^2},$$

where v *and* V_i *denotes the exact and numerical solution respectively at the node point* x_i *for some fixed time.*

Example 1. *The generalized Rosenau-KdV equation (1)is considered for* $\alpha = 1$, $\beta = 0.5$ *and* $\gamma = 1$*:*

$$v_{xxxxT} + v_{xxx} + (0.5)(v^2)_x + v_T + v_x = 0, \quad (x,T) \in [-70, 100] \times (0, 20] \tag{5.1}$$

In this equation power nonlinearity $p = 2$*. The exact solitary wave solution of eq.(5.1) obtained by [36] is given as follows:*

$$v(x,T) = \mathfrak{K}_1 sech^4(\mathfrak{K}_2(x - \mathfrak{K}_3 t)) \tag{5.2}$$

where
$\mathfrak{K}_1 = -\frac{35}{24} + \frac{35\sqrt{313}}{312}$, $\mathfrak{K}_2 = \frac{1}{24}\sqrt{-26 + 2\sqrt{313}}$ *and* $\mathfrak{K}_3 = \frac{1}{2} + \frac{\sqrt{313}}{26}$.

Comparison of L_2 *error norm is shown in Table 1 over the spatial domain* $\Upsilon = [-70, 100]$ *at time* $T = 20$ *with different spatial and temporal step sizes* $h = \Delta T$*. Table 2 presents the* L_∞ *error norm for the same set of parameter values at various time levels. Table 3 and Table 4 shows comparison of order of convergence corresponding to* L_2 *and* L_∞ *error norm at* $T = 20$ *for* $h = \Delta T$ *respectively. The numerical simulations obtained by CFDM6 are compared with implicit finite difference scheme [23], linear implicit finite difference [36], time-splitting techniques quintic B-spline collocation method [30] shows a frightening accuracy, with the highest order of convergence.*

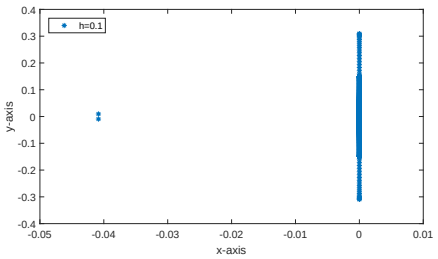

(a) $h = 0.1$

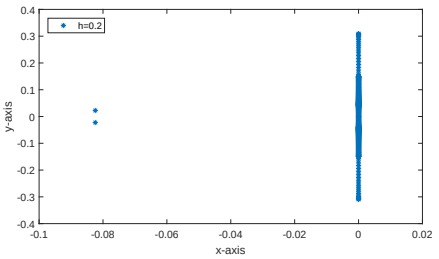

(b) $h = 0.2$

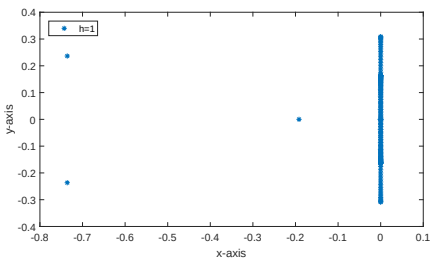

(c) $h = 1$

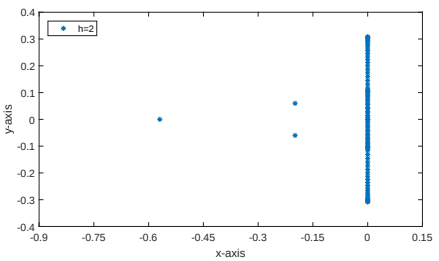

(d) $h = 2$

Figure 2: Ratio of eigenvalues of Problem 1 for various spatial increment sizes h and $T = 20$.

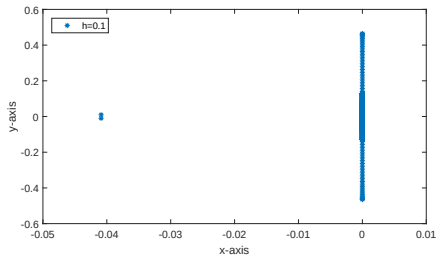

(a) $h = 0.1$

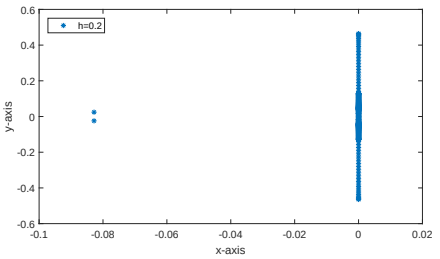

(b) $h = 0.2$

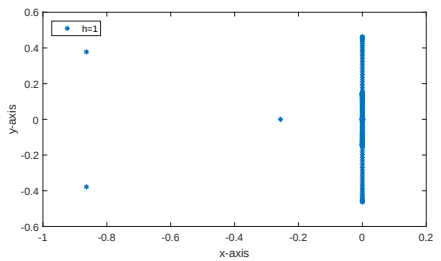

(c) $h = 1$

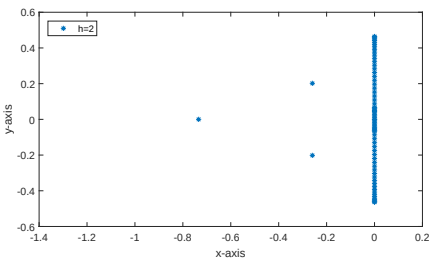

(d) $h = 2$

Figure 3: Eigenvalues of Problem 2 for various spatial increment sizes h and $T = 20$.

A comparison with quoted methods for discrete energy and mass at different times $t = 0, 10, 20$ *is shown in Table 5. The invariants remain constant throughout the time domain depicting the conservation. Figure 4 represents the exact and numerical solution at different time levels* $t = 0, 5, 10, 15, 20$. *The numerical results are seen in good agreement with exact solutions. In figure 4 numerical solutions is seen in the surface plotting. The conservation properties are also preserved as the invariants remain almost constant at different time values.*

Table 1: L_2 error norm comparison of Example 1 at $T = 20$ for various values of $h = \Delta T$.

$h = \Delta T$	AIFDS [23]	LIFDS [44]	Strang [45]	Lie–Trotter[45]	CFDM6
0.2	1.7780e-03	9.0022e-04	0.9663e-04	0.3594e-02	5.7276e-05
0.1	4.4396e-04	1.1334e-04	0.2418e-04	0.1798e-02	7.1744e-06
0.05	1.1098e-04	1.4196e-05	0.6046e-05	0.8997e-03	8.9768e-07
0.025	2.7748e-05	1.7757e-06	0.1514e-05	0.4500e-03	1.1868e-07

Table 2: L_∞ error norm comparison of Example 1 at $T = 20$ for various values of $h = \Delta t$.

$h = \Delta T$	AIFDS [23]	LIFDS [44]	Strang [45]	Lie–Trotter[45]	CFDM6
0.2	4.9510e-04	7.8920e-04	0.3569e-04	0.1055e-02	7.7337e-06
0.1	1.2373e-04	1.8771e-04	0.0893e-04	0.5303e-03	1.1751e-05
0.05	3.0934e-05	4.6987e-05	0.2234e-05	0.2659e-03	3.4328e-07
0.025	2.7748e-05	1.7757e-06	0.0560e-05	0.1331e-03	3.9667e-08

Table 3: Order of convergence of Example 1 is compared for L_2 error norm at $T = 20$ for various values of $h = \Delta T$.

$h = \Delta t$	CFDM6	AIFDS [23]	LIFDS [44]	Lie–Trotter [45]	Strang [45]
0.025	2.9191	1.9999	1.99908	0.9996	1.9976
0.05	2.9986	2.0001	1.99710	0.9993	1.9997
0.1	2.9970	2.0017	1.98959	0.9987	1.9988
0.2	-	-	-	-	-

Table 4: Order of convergence of Problem 1 is compared for L_∞ error norm at $T = 20$ for various values of $h = \Delta T$.

$h = \Delta T$	CFDM6	AIFDS [23]	LIFDS [44]	Lie–Trotter [45]	Strang [45]
0.025	3.1134	2.0000	1.9995	0.9984	1.9961
0.05	3.0011	1.9999	1.9982	0.9959	1.9990
0.1	3.0000	2.0005	2.0719	0.9924	1.9998
0.2	-	-	-	-	-

Table 5: Conservative mass and energy invariants of Example 1 are compared.

$(h, \Delta T)$	Scheme		$T = 0$	$T = 10$	$T = 20$
(0.1,0.1)	CFDM6	$\mathcal{Q}$	5.49817368082	5.49817368081	5.49817368080
		$\mathcal{E}$	1.98433571815	1.98978063915	1.98977833762
	Lie–Trotter [45]	$\mathcal{Q}$	5.49817368082	5.49817368167	5.49817368131
		$\mathcal{E}$	1.98978293967	1.98978295070	1.98978294643
	Strang [45]	$\mathcal{Q}$	5.49817368082	5.49817368083	5.49817368082
		$\mathcal{E}$	1.98978293967	1.98978293985	1.98978293963
(0.05.0.025)	CFDM6	$\mathcal{Q}$	5.49817368082	5.49817368078	5.49817368070
		$\mathcal{E}$	1.98433571815	1.98978282455	1.98978265185
	Lie–Trotter [45]	$\mathcal{Q}$	5.49817368082	5.49817368083	5.49817368089
		$\mathcal{E}$	1.98978293960	1.98978293998	1.98978293983
	Strang [45]	$\mathcal{Q}$	5.49817368083	5.49817367978	5.49817368085
		$\mathcal{E}$	1.98978293963	1.98978293987	1.98978293963

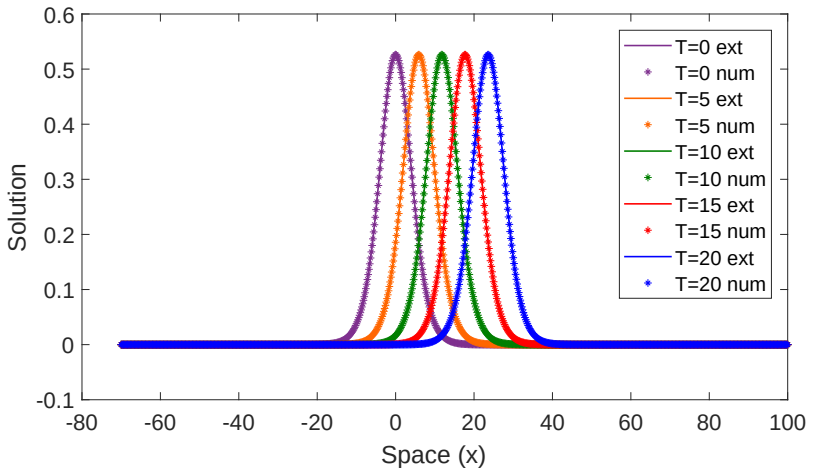

Figure 4: Exact and Numerical solutions are compared for Example 1 with $h = \Delta T = 0.2$ at various times.

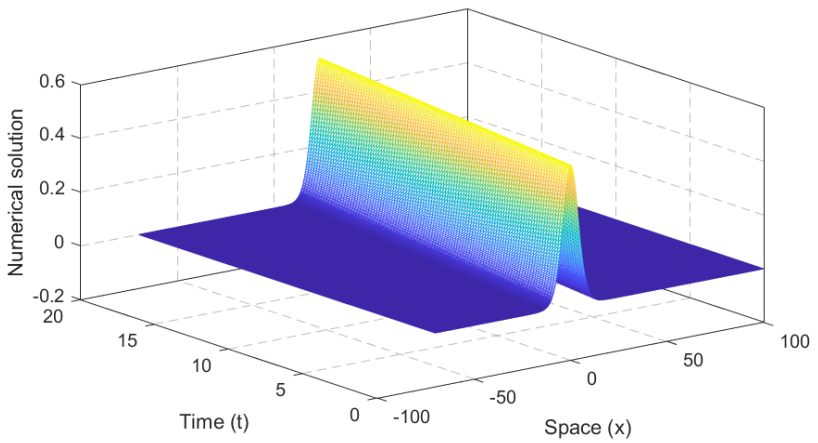

Figure 5: Numerical solution of Example 1 with $h = \Delta T = 0.2$ for given $T = 20$ in surface plot.

Example 2. *Consider the invariants α, β and γ as unity and power law nonlinearity $p = 5$. The following equation is obtained:*

$$v_{xxxxT} + v_{xxx} + (v^5)_x + v_x + v_T = 0, \quad (x, T) \in [-60, 90] \times (0, 40] \tag{5.3}$$

where the initial condition is given by:

$$v(x, T) = \mathfrak{c}_1 sech(\mathfrak{c}_2 x), \quad x \in [-60, 90] \tag{5.4}$$

and the boundary conditions are:

$$\begin{aligned} v[-60, T] = v[90, T] = 0, \\ v_x[-60, T] = v_x[90, T] = 0, \\ v_{xx}[-60, T] = v_{xx}[90, T] = 0 \end{aligned} \tag{5.5}$$

The exact solitary wave solution was obtained by [36] as follows:

$$u(x, T) = \mathfrak{c}_1 sech(\mathfrak{c}_2 (x - \mathfrak{c}_3 T)) \tag{5.6}$$

where $\mathfrak{c}_1 = \left(\frac{4}{15}(-5+\sqrt{34})\right)^{\frac{1}{4}}$, $\mathfrak{c}_2 = \frac{1}{3}\sqrt{-5+\sqrt{34}}$ *and* $\mathfrak{c}_3 = \frac{1}{10} + (5+\sqrt{34})$.

*Table 7 displays the comparison of L_2 error norm over the spatial domain $[-60, 90]$ at time $T = 40$ for varying spatial and temporal size with $h = \Delta T$. Table **??** displays the comparison of L_∞ error norm over the same spatial and temporal domain. It is clearly seen that numerical simulation by CFDM6 are in good agreement with exact solutions. Comparison shown in Table 8 and Table 9 depicts the order of convergence of L_2 and L_∞ error norm at $T = 40$ respectively for the same parametric nature $h = \Delta t$ at intermediate time levels. Tabular representation of numerical simulations obtained by CFDM6, implicit finite difference scheme [23], linear implicit finite difference [36], time-splitting techniques quintic B-spline collocation method [30] shows highest order of convergence. An awful accuracy is demonstrated depicting an proximity between exact and numerical solutions.*

Table 10 shows comparison of computed discrete energy and mass at different times $t = 0, 20, 40$ for space and time steps $h = \Delta T = 0.25$ and $h = \Delta T = 0.125$. The conservation of the invariants is analyzed over the time span. Figure 6 presents the correlation between numerical and exact solution at various time levels $T = 0, 10, 20, 30, 40$. The solution computed with present method are shown in surface plots in figure 7 over a time span $[-60, 90]$ with $h = \Delta T = 0.125$. The wave amplitude remain same at different time values, showing the invariants remain constant and preserved over run time.

Table 6: L_2 error norm of Example 2 are compared at $T = 40$ for various values of $h = \Delta T$.

$h = \Delta T$	Lie–Trotter [45]	Strang [45]	CFDM6
0.25	0.9454e-02	0.1495e-02	1.0234e-03
0.125	0.4631e-02	0.3743e-03	1.3158e-04
0.0625	0.2297e-02	0.0936e-03	1.6708e-05
0.03125	0.1145e-02	0.2346e-04	2.4311e-06

Table 7: L_∞ error norm of Example 2 are compared at $T = 40$ for various values of $h = \Delta T$.

$h = \Delta T$	AIFDS [23]	LIFDS [44]	Lie–Trotter [45]	Strang [45]	IFDS [46]	CFDM6
0.25	1.7998e-02	9.2311e-03	0.2756e-02	0.5711e-03	7.7054e-03	3.8560e-04
0.125	4.5680e-03	2.3321e-03	0.1277e-02	0.1430e-03	1.9425e-03	4.9458e-05
0.0625	1.1469e-03	5.8475e-04	0.6136e-03	0.3578e-04	4.8655e-04	6.2547e-06
0.03125	2.8708e-04	1.4633e-04	0.3006e-03	0.0895e-04	1.2170e-04	1.0021e-06

Table 8: Convergence order comparison for L_2 of Example 2 at $T = 40$ for various estimates with $h = \Delta T$.

$h = \Delta T$	Lie–Trotter [45]	Strang [45]	CFDM6
0.25	-	-	-
0.125	1.0297	1.9976	2.9595
0.0625	1.0115	1.9992	2.9773
0.03125	1.0049	1.9967	2.7809

Table 9: Convergence order comparison for L_∞ of Example 2 at $T = 40$ for various estimates with $h = \Delta T$.

$h = \Delta T$	AIFDS [23]	IFDS [46]	LIFDS [44]	Lie–Trotter [45]	Strang [45]	CFDM6
0.25	-	-	-	-	-	-
0.125	1.9782	1.9879	1.9849	1.1095	1.9972	2.9628
0.0625	1.9938	1.9973	1.9957	1.0578	1.9993	2.9832
0.03125	1.9982	1.9993	1.9986	1.0295	1.9998	2.6390

Table 10: Energy invariants and conservative mass of Example 2 are compared.

T	Scheme	$h = \Delta T = 0.25$		$h = \Delta T = 0.125$	
		$\mathcal{Q}$	$\mathcal{E}$	$\mathcal{Q}$	$\mathcal{E}$
T=0	CFDM6	7.09364313608	3.09838667696	7.09364313713	3.09838667696
	Lie–Trotter [45]	7.09364314022	3.11071232837	7.09364313921	3.11071230874
	Strang [45]	7.09364314022	3.11071232837	7.09364313921	3.11071192879
T=20	CFDM6	7.09364324499	3.11061204597	7.09364323831	3.11069974244
	Lie–Trotter [45]	7.09364340837	3.11071270609	7.09364315594	3.11071238684
	Strang [45]	7.09364302323	3.11071217839	7.09364309672	3.11071230891
T=40	CFDM6	7.09364333648	3.11051170008	7.09364332285	3.11068716975
	Lie–Trotter [45]	7.09352321531	3.11051170008	7.09358149621	3.11071235544
	Strang [45]	7.09364013713	3.11071192879	7.09364113290	3.11071230277

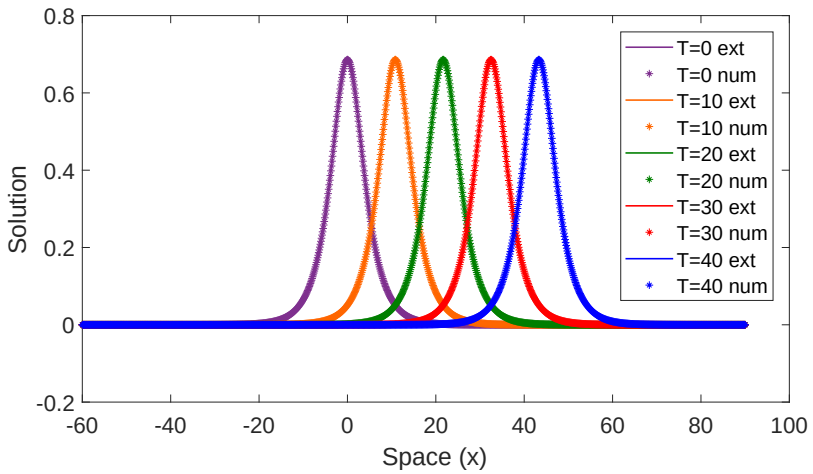

Figure 6: Exact and Numerical solutions of Example 2 are compared with $h = \Delta T = 0.125$ at various times.

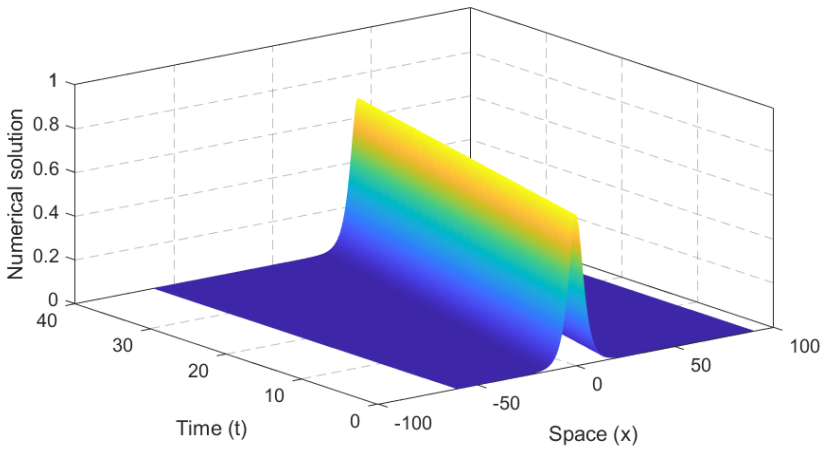

Figure 7: Numerical solution of Example 2 with $h = \Delta T = 0.125$ and $T = 40$ surface plot.

6 Conclusion

This study focused on the numerical solution of the generalized Rosenau-KdV equation employing CFDM6 in conjunction with the SSP-RK43 scheme. The values, along with the corresponding initial and boundary conditions, are calculated exclusively. The numerical solutions, as well as the L_2 and L_∞ error norms computed using CFDM6, are remarkably impressive. The results achieved are highly promising when compared to other numerical methods documented in the literature. Furthermore, the discrete mass and energy are maintained, which is a crucial aspect for any technique's effectiveness and precision. Stability analysis indicates that the proposed method is stable for this nonlinear partial differential equation. Therefore, it is concluded that this method is accurate, effective, and demonstrates a higher order of convergence. Future scope of this method is its application to time factional problems.

References

[1] *P.F.Zhao and M.Z. Qin,* Multisymplectic geometry and multisymplectic Preissmann scheme for the KdV equation, *J. Phys. A Math. Gen.*, **33**, *3613–3626, (2000).*

[2] *Yan, J. and C.W. Shu,* A local discontinuous Galerkin method for KdV type equations, *SIAM J. Numer. Anal.*, **40**, *769–791, (2002).*

[3] *A. Korkmaz,* Numerical algorithms for solutions of Korteweg-de Vries equation, *Numerical methods for partial differential equations,* **26**, *1504–1521, (2010).*

[4] *H. Holden, K. Karlsen, N. Risebro and T. Tao,* Operator splitting for the KdV equation, *Math. Comput.*, **80**, *821–846, (2011).*

[5] *N.A. Kudryashov,* Painleve analysis and exact solutions of the Korteweg-de Vries equation with a source, *Appl. Math. Lett.*, **41**, *41–45, (2015).*

[6] *H.Triki, T. Ak, S. Moshokoa and A. Biswas,* Soliton solutions to KdV equation with spatio-temporal dispersion, *Ocean Eng.*, **114**, *192–203, (2016).*

[7] *Attia, R.A., Xia, Y., Zhang, X. and Khater, M.M.,*Analytical and numerical investigation of soliton wave solutions in the fifth-order KdV equation within the KdV-KP framework, *Results Phys.*, **51**, *1–12, 2023.*

[8] *Pandir, Y. and Ekin, A.,* New solitary wave solutions of the Korteweg-de Vries (KdV) equation by new version of the trial equation method, *Electron. J. Appl. Math.*, **1**, *101–113, 2023.*

[9] *Ma, W.X.,* A polynomial conjecture connected with rogue waves in the KdV equation, *Partial Differ. Equ. Appl. Math.*, **3**, *1–3, 2021.*

[10] *P. Rosenau,* Dynamics of dense discrete systems: high order effects, *Prog. Theor. Phys.*, **79**, *1028–1042, (1988).*

[11] *M.A. Park,* On the Rosenau equation, *Comput. Appl. Math.*, **9**, *145–152, (1990).*

[12] *M.A. Park,* Pointwise Decay Estimate of Solutions of the Generalized Rosenau Equation, *Journal of the Korean Mathematical Society,* **29**, *261–280, (1992).*

[13] S. K. Chunk and A. K. Pani, Numerical methods for the rosenau equation: Rosenau equation, *Appl. Anal.,* **77**, *351-369, (2001).*

[14] S. M. Choo, S. K. Chung and K. I. Kim, A discontinuous Galerkin method for the Rosenau equation, *Appl. Numer. Math.,* **58**, *783–799, (2008).*

[15] S. K. Chung, Finite Difference Approximate Solutions for: the Rosenau Equation, *Appl. Anal.,* **69**, *149–156, (1998).*

[16] S. A. V. Manickam, A. K. Pani and S. K. Chung, A second-order splitting combined with orthogonal cubic spline collocation method for the Rosenau equation, *Numer. Meth. Part Differ. Equ.,* **14**, *695–716, 1998.*

[17] K. Omrani, F. Abidi, T. Achouri and N. Khiari, A new conservative finite difference scheme for the Rosenau equation, *Appl. Math. Comput.,* **201**, *35-43, (2008).*

[18] N. Atouani and K. Omrani, A new conservative high-order accurate difference scheme for the Rosenau equation, *Appl. Anal.,* **94**, *2435–2455, (2015).*

[19] N. Atouani, Y. Ouali and K. Omrani, Mixed finite element methods for the Rosenau equation, *J. Appl. Math. Comp.,* **57**, *393–420, (2018).*

[20] A. Safdari-Vaighani, E. Larsson, and A. Heryudono, Radial basis function methods for the Rosenau equation and other higher order PDEs, *J. Sci. Comput.,* **75**, *1555–1580, (2018).*

[21] J. M. Zuo, Solitons and periodic solutions for the Rosenau-KdV and Rosenau-Kawahara equations, *Appl. Math. Comput.,* **215**, *835–840, (2009).*

[22] A. S. I. T. Saha, Topological 1-soliton solutions for the generalized Rosenau-KdV equation, *Fundam. J. Math. Phys.,* **2**, *19–23,(2012).*

[23] B. Wongsaijai and K. Poochinapan, A three-level average implicit finite difference scheme to solve equation obtained by coupling the Rosenau-KdV equation and the Rosenau-RLW equation, *Appl Math Comput.,* **245**, *289–304, (2014).*

[24] X. Wang and W. Dai, A conservative fourth-order stable finite difference scheme for the generalized Rosenau-KdV equation in both 1D and 2D. *J. Comput. Appl. Math.,* **355**, *310–331, (2019).*

[25] W. Cai, Y. Sun and Y. Wang, Variational discretizations for the generalized Rosenau-type equations, *Appl Math Comput.,* **271**, *860–873, (2015).*

[26] T. Ak, S. B. G. Karakoc and H. Triki, Numerical simulation for treatment of dispersive shallow water waves with Rosenau-KdV equation, *Eur. Phys. J. Plus.,* **131**, *1–15, (2016).*

[27] T. Ak, S. Dhawan, S.B.G. Karakoc, S.K. Bhowmik and K.R. Raslan, Numerical study of Rosenau-KdV equation using finite element method based on collocation approach, *Math. Model. Anal.,* **22**, *373–388, (2017).*

[28] J. Hu, J. Zhou and R. Zhuo, A high-accuracy conservative difference approximation for Rosenau-KdV equation, *J. Nonlinear Sci. Appl.,* **10**, *1–15, (2017).*

[29] S.B.G. Karakoc, A detailed numerical study on generalized Rosenau-KdV equation with finite element method, *J. Sci. Arts.,* **18**, *837–852, (2018).*

[30] S. Kutluay, M. Karta, N. M. Yagmurlu, Operator time-splitting techniques combined with quintic B-spline collocation method for the generalized Rosenau-KdV equation, *Numer. Methods Partial Differ. Equ.,* **35**, *2221–2235, (2019).*

[31] M. Hussain and S. Haq, Numerical simulation of solitary waves of Rosenau-KdV equation by Crank-Nicolson meshless spectral interpolation method, *Eur. Phys. J. Plus.,* **135**, *98–111, (2020).*

[32] Oruc,O., Esen, A. and Bulut, F., Numerical Solution of the Rosenau-KdV-RLW equation via combination of a polynomial scaling function collocation and finite difference method, *Math. Methods Appl. Sci.,* **2024**, *1–20, 2024.*

[33] S.K. Lele, Compact finite difference schemes with spectral-like resolution, *J. Comput. Phys.,* **103**, *16–42, (1992).*

[34] D. Li, C. Zhang and J. Wen, A note on compact finite difference method for reaction-diffusion equations with delay, *Appl. Math. Model.,* **39**, *1749–1754, (2015).*

[35] H. Wang, Y. Zhang, X. Ma, J. Qiu and Y. Liang, An efficient implementation of fourth-order compact finite difference scheme for Poisson equation with Dirichlet boundary conditions, *Comput. Math. Appl.,* **71**, *1843–1860, (2016).*

[36] H. Wang, X. Ma, J. Lu and W. Gao, An efficient time-splitting compact finite difference method for Gross-Pitaevskii equation, *Appl. Math. Comput.,* **297**, *131–144, (2017).*

[37] L. Li, Z. Jiang and Z. Yin, Fourth-order compact finite difference method for solving two-dimensional convection-diffusion equation, *Adv. Differ. Equ.,* **2018**, *234–258, (2018).*

[38] H. Liu, A. Cheng, H. Yan, Z. Liu and H. Wang, A fast compact finite difference method for quasilinear time fractional parabolic equation without singular kernel, *Int. J. Comput. Math.,* **96**, *1444–1460, (2019).*

[39] Y. Huang and Z. Yin, The Compact Finite Difference Method of Two-Dimensional Cattaneo Model*, J. Funct. Spaces,* **2020***, 1–12, (2020).*

[40] P. Roul and V.P. Goura, A new higher order compact finite difference method for generalised Black-Scholes partial differential equation: European call option*, J. Comput. Appl. Math.,* **363***, 464–484, (2020).*

[41] D.V. Gaitonde and M.R. Visbal, High-order schemes for Navier-Stokes equations: algorithm and implementation into FDL3DI (No. AFRL-VA-WP-TR-1998-3060)*, Air Force Research Lab Wright-Patterson AFB OH Air Vehicles Directorate, (1998).*

[42] M.K. Jain, Numerical solutions of differential equations: Wiley Eastern Ltd*, (1984).*

[43] E.J. Kubatko, B.A. Yeager and D.I. Ketcheson, Optimal strong-stability-preserving Runge-Kutta time discretizations for discontinuous Galerkin methods*, J. Sci. Comput.,* **60***, 313–344, (2014).*

[44] X. Wang and W. Dai, A three-level linear implicit conservative scheme for the Rosenau-KdV-RLW equation*, J. Comput. Appl. Math.,* **330***, 295–306, (2018).*

[45] S. Kutluay, M. Karta and N.M. Yagmurlu, Operator time-splitting techniques combined with quintic B-spline collocation method for the generalized Rosenau-KdV equation*, Numer. Methods Partial Differ. Equ.,* **35***, 2221–2235, (2019).*

[46] J. Zhou, M. Zheng and R.X. Jiang, The conservative difference scheme for the generalized Rosenau-KDV equation*, Therm. Sci.,* **20***, 903–910, (2016).*

Author information

Ravneet Kaur, Department of Mathematics, Rayat Bahra University, Mohali, India.
E-mail: kaur.ravneet08@gmail.com

V.K.Kukreja, Department of Mathematics, SLIET, Longowal, India.
E-mail: vkkukreja@gmail.com